Available online at www.sciencedirect.com

SCIENCE DIRECT®

Cement and Concrete Research 35 (2005) 1368–1376

Cement and Concrete Research

Influence of lightweight aggregate on the microstructure and durability of mortar

Amir Elsharief[a,*], Menashi D. Cohen[b], Jan Olek[b]

[a]Department of Civil Engineering and Construction, Bradley University, 1501 W. Bradley Avenue, Peoria, IL 61625, United States
[b]School of Civil Engineering, Purdue University, 1284 Civil Engineering Building, G217, West Lafayette, IN 47907, United States

Received 10 October 2003; accepted 8 July 2004

Abstract

The results of an investigation on the effect of dry and prewetted lightweight aggregates on the microstructure and durability of mortar are presented in this paper. The results are compared with those obtained for normal aggregate mortar. There appears to be only a small difference in the microstructure of the interfacial transition zone (ITZ) between dry and prewetted lightweight aggregate mortars. The porous ITZ surrounding lightweight aggregate appears to extend for about 10 and 15 μm from the aggregate surface for dry and prewetted lightweight aggregates, respectively. The ITZ for dry and prewetted lightweight aggregates seems to be surrounded by dense paste that extends from 10 to about 50 μm from the aggregate surface. This dense paste has lower porosity than that observed in the bulk paste located 50 μm and farther from aggregate surface. The normal aggregate mortar prepared with the same water/cement ratio appears to have porous ITZ that extends beyond 35 μm from the aggregate surface. The dry and prewetted lightweight aggregate mortars seem to have a lower sorptivity and electrical conductivity than does the normal aggregate mortar. Lightweight aggregate mortars also appear to have excellent resistance to sulfate attack as compared with normal aggregate mortar.

Keywords: Interfacial transition zone; SEM; Durability; Aggregate; Sulfate attack

1. Introduction

Several researchers have suggested that lightweight aggregate absorbs water from the surrounding paste, leading to a reduction in the porosity of the interfacial transition zone (ITZ) surrounding the aggregate. Zhang and Giorv [1,2] examined the ITZ microstructure around expanded clay lightweight aggregate. The study included lightweight aggregate with and without dense outer layer. The aggregate with dense outer layer showed porous ITZ microstructure similar to the one observed around the normal-weight aggregate. As for the lightweight aggregate with porous outer layer, the ITZ was more dense and homogeneous. Wasserman and Bentur [3,4] studied the ITZ around lightweight sintered fly ash aggregate. The aggregate was modified by sintering at various high temperatures. By so doing, the vitrification takes place, and a dense surface is produced. The sintering process produced lightweight aggregates with different water absorptions and crushing strengths. The ITZ width was estimated by measuring the calcium/silica ratio using dispersive X-ray spectroscopy. The lightweight aggregate with the highest absorption capacity showed ITZ of very small thickness. The thickness of the ITZ appeared to decrease linearly with the absorption capacity of the aggregate. The heat-treated aggregate acquired pozzolanic reactivity proportional to the amount of heat applied. The pozzolanic activity was attributed to the formation of a glassy phase of silica (SiO_2). The pozzolanic reaction between the aggregate and the calcium hydroxide resulted in a reduction in the calcium/silica ratio in the ITZ to the level observed in the bulk paste after 90 days of curing. Sarkar et al. [5]

* Corresponding author. Tel.: +1 309 677 2551; fax: +1 309 677 2867.
E-mail address: aelsharief@bradley.edu (A. Elsharief).

0008-8846/$ - see front matter © 2004 Elsevier Ltd. All rights reserved.
doi:10.1016/j.cemconres.2004.07.011

confirmed the results obtained by Gjørv concerning the outer layer of the aggregate. However, the researchers could not find any evidence of the pozzolanic reaction between the aggregate and the cement paste. Lo et al. [6] studied the microstructure of the ITZ between lightweight aggregate and the cement paste. Their findings confirmed the presence of dense ITZ microstructure. They suggested that the improvement in the ITZ microstructure was probably due to the absorption of water by the lightweight aggregate from the paste. Holm et al. [7] investigated the microstructure of the ITZ in mature lightweight aggregate concrete obtained from concrete ships and marine structures using scanning electron microscopy. They concluded that the contact zone between the continuous matrix and the coarse aggregate is essentially indistinguishable at the transition zone between the two phases. They attributed the enhancement of the ITZ microstructure to the pozzolanic reaction of the lightweight aggregate and absorption of water by lightweight aggregate.

The positive impact that the lightweight aggregate has on the microstructure of the ITZ appears to improve the transport properties and durability of mortar and concrete. Punkki and Gjørv [8] and Punkki et al. [9] conducted a study on the effect of lightweight aggregate moisture treatment on the ITZ microstructure and water absorption of concrete. Concrete samples with water/cement ratio of 0.35 and 7% silica fume and water/cement ratio of 0.42 without silica fume were prepared. The aggregates used were either dry or soaked in water for 24 h. The absorption test results indicated that prewetted lightweight aggregate concrete has slightly higher capillary suction or absorption. The increase in absorption was attributed to the porous ITZ microstructure around the prewetted lightweight aggregate as compared with the ITZ around the dry aggregate. Chia and Zhang [10] investigated the effect of aggregate type on the water permeability of concrete. Concrete specimens with lightweight and normal aggregate were prepared. The results indicated that the permeability of lightweight aggregate concrete was lower than that of the normal aggregate concrete. The lower permeability of lightweight aggregate concrete was thought to be due to the denser ITZ around the lightweight aggregate as compared with the normal weight aggregate.

In this study, the effect of dry and prewetted lightweight aggregates on the ITZ microstructure was examined and quantified by using backscattered electron microscopy (BSE) mode of the scanning electron microscope (SEM) and image analysis. The microstructural features investigated in this study were porosity and unhydrated cement (UH) grains content. The microstructure of the ITZ around the lightweight aggregate was compared with that around the normal aggregate. The effect of lightweight aggregate on the porosity, sorptivity and electrical conductivity of mortar, as well as resistance to sulfate attack, was also investigated in this study.

2. Experimental

2.1. Materials, mixing and casting

The lightweight aggregate used in this study was Haydite, which was manufactured by expanding shale in a rotary kiln, from Brooklyn, IN. It was crushed and sieved into single gradation passing sieve #50 and retained on sieve #100 (300–150 μm). The specific gravity and absorption values for this gradation, obtained by the procedure described in ASTM C 128, were determined to be 2.0 and 7%, respectively.

The lightweight aggregate described above was used to prepare mortar specimens with w/c of 0.55 and ASTM type I portland cement. The characteristic of ASTM type I portland cement used in the mixtures is given in Table 1. Prior to mixing, the lightweight aggregate was dried in an oven at 105 °C for 2 days. At the end of the drying period, the aggregate was allowed to cool down to room temperature. Two sets of mortar were prepared. The first set was prepared with dry lightweight aggregate. Mixing was done according to the procedure described in ASTM C 305, except that the time for the last mixing interval was increased from 1 to 4 min. The second set was prepared with prewetted lightweight aggregate soaked in the mix water for 24 h prior to mixing. The mix water and the lightweight aggregate soaked in it were covered with plastic sheets and wet burlap to avoid loss of water through evaporation. Mixing was done by starting the mixer and adding cement slowly during the first minute. The rest of the mixing procedure conformed to ASTM C 305, except that the time for the last mixing interval was increased from 1 to 4 min. All mortars were mixed in a Hobart mortar mixer with a 13,500-ml capacity. The volume fraction of the aggregate used in the two sets of mortars was 40% of the total mixture volume. The amount of water to be absorbed by the aggregate was calculated, based on 7% absorption, and added to the mix water to give an effective w/c of 0.55. The mixture proportions are provided in Table 2.

Table 1
Characteristics of ASTM type I Portland cement used in the mixtures

CaO	SiO_2	Al_2O_3	Fe_2O_3	MgO	SO_3	Na_2O	K_2O	TiO_2	P_2O_5	Mn_2O_3	SrO
64.2	20.28	5.37	2.40	1.81	3.36	0.07	0.80	0.30	0.09	0.04	0.07

Table 2
Mixture proportions for lightweight and normal aggregate mortars

Series	w/c	Water (kg/m^3)	Cement (kg/m^3)	Sand (kg/m^3)	Sand volume (%)
Light–dry	0.55	436	691	804	40
Light–dry	0.55	436	691	804	40
Normal	0.55	380	691	1060	40

Siliceous normal weight aggregate of the same gradation as the lightweight aggregate was used to prepare mortar with similar mixture proportions. The details of preparation of the siliceous normal weight aggregate mortar are provided in reference [11]. The mixture proportions for the siliceous normal weight aggregate mortar are given in Table 2.

2.2. Specimens preparation and testing

2.2.1. SEM specimens and image acquisition

SEM samples were cut off from a 1×1×12 in. prism stored in lime water. The samples were 7 days old when they were processed. The details of the procedure for the SEM specimens' preparation and image acquisition and analysis are given in Ref. [11].

2.2.2. Absorption

Cylindrical specimens with 68-mm diameter and 151-mm length were cast using lightweight and normal aggregate mortars. The cylinders were cured in lime water. At ages of 7 and 180 days, 25-mm-thick discs were sliced from these cylinders using diamond saw. Immediately after slicing, the discs were subjected to vacuum saturation in water for 8 h and then left in water for an additional 16 h. The saturated surface dry weight was recorded at the end of the soaking period. The specimens were then placed in an oven set at 105 °C for 72 h. The dry weight was determined, and the absorption was calculated based on the dry weight.

2.2.3. Sorptivity

To determine sorptivity, 25-mm-thick discs were sliced from cylinders of 68-mm diameter and 151-mm length at the age of 180 days. The discs were stored in an oven set at 50 °C until constant weight was reached. It took approximately 30 days to achieve stable mass. This treatment removed most of the evaporable water from the capillary pores and did not appear to induce significant damage that might otherwise affect the test results. Protective coating was applied to the circumference of the discs to prevent water from penetrating through the sides. The specimens were weighed, and then one face was placed in contact with water. The gain in weight due to water absorption was measured at 5-min intervals for a period of 40 min. The sorptivity was obtained by plotting the gain in weight per unit area versus the square root of time. The relationship between these two parameters is linear, and the slope of the line was considered as the parameter describing the sorptivity.

2.2.4. Electrical conductivity

A conductivity test developed by Streicher and Alexander [12] was used in this study. The specimens used were discs of 68-mm diameter and 25-mm thickness. The specimens were dried in a similar way as mentioned in the previous section, after 7 and 180 days of curing in lime water. They were then vacuum saturated in 5 M NaCl solution. DC current passing through the specimen at a given voltage was recorded. The conductivity was calculated based on the following equation:

$$\sigma = \frac{i}{v}\frac{t}{A} \tag{1}$$

where σ=conductivity of sample (mS/cm); i=electric current (mA); v=potential difference (V); t=thickness of sample (cm); and A=cross-sectional area of the sample (cm^2).

2.2.5. Sulfate attack

After 14 days of curing in lime water, 1×1×11.25 in. (2.54×2.54×28.57 cm) prisms fitted at the ends with stainless steel studs were immersed in 5% Na_2SO_4 solution. The expansion and dynamic modulus were measured periodically. The SO_3 concentration profile was obtained by using energy dispersive X-ray spectroscopy (EDS). The X-ray spectrum was obtained from polished specimens at equal intervals staring from the specimen surface. The quantitative analysis of the oxides percentages was performed by using Flame software.

3. Results and discussion

3.1. Microstructure

The BSE micrographs for the paste surrounding the dry and prewetted lightweight aggregates, as well as normal aggregate, are shown in Fig. 1(a), (b) and (c). The porosity of the ITZ around the lightweight and normal aggregate, expressed as a function of distance from the aggregate surface, is shown in Fig. 2. The bulk paste porosity also is presented in Fig. 2 by a point outside the range of the horizontal scale. The results indicate that for the 10-μm strip in the immediate vicinity of the aggregate, the prewetted lightweight aggregate has the highest porosity. The normal aggregate porosity for the same strip is lower than that of prewetted lightweight aggregate but higher than that of the dry lightweight aggregate. This difference in the porosity of the first 10 μm around the three different aggregates can be attributed to the absorption capacity of the aggregate. The dry lightweight aggregate possesses higher absorption capacity than the normal and prewetted lightweight aggregate does. Thus, the bleed water was

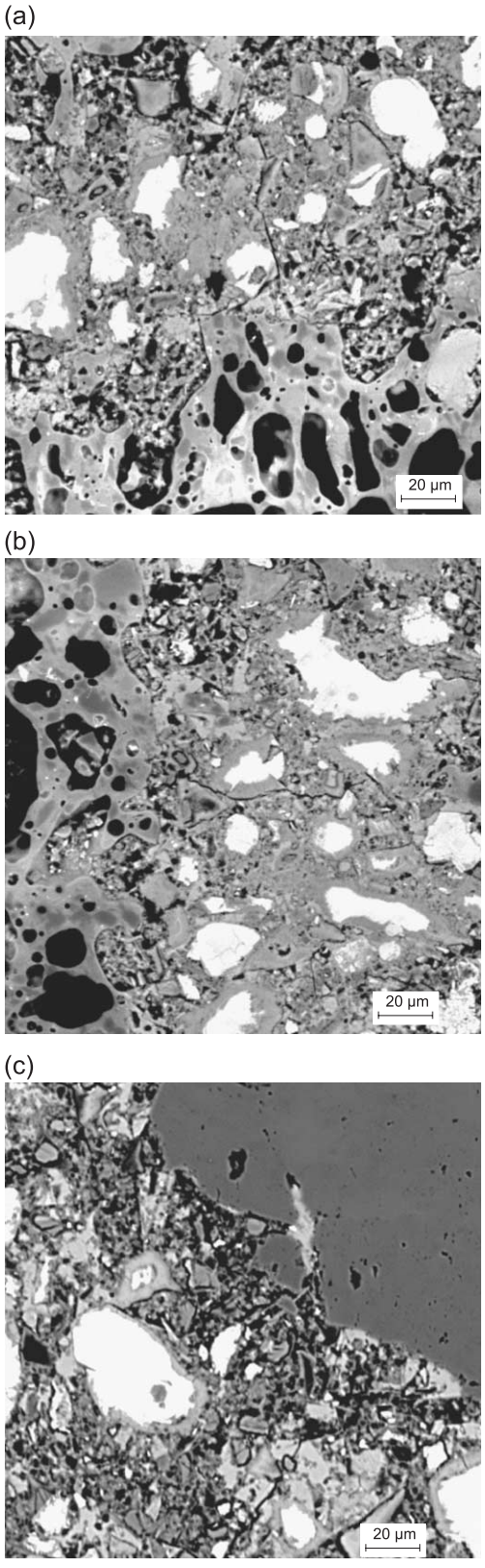

Fig. 1. (a) Paste surrounding dry lightweight aggregate at 7-day age. (b) Paste surrounding prewetted lightweight aggregate at 7-day age. (c) Paste surrounding normal aggregate at 7-day age.

reduced more significantly in this case. The dry, normal aggregate appears to reduce the bleed water in the first 10-μm strip surrounding the aggregate more efficiently than prewetted lightweight aggregate does. However, despite the difference in porosity between the three aggregates in the 10-μm strip immediately surrounding the aggregate, the porosity is still significantly higher than that of the bulk paste. This may indicate that bleeding around the aggregate at a w/c of 0.55 cannot be completely eliminated by absorbing water by the aggregate. At the distance between about 10 and 40 μm from the aggregate surface, the porosity of the paste surrounding the dry lightweight aggregate appears to be significantly smaller than that of the paste surrounding the normal aggregate. For the dry lightweight aggregate, the porosity of the paste located between 10 and 40 μm from the aggregate surface is even lower than that of the bulk paste. This reduction in porosity may be attributed to the absorption of water by the lightweight aggregate. The process of water bleeding and absorption can be described as follows. When the aggregate is mixed with cement and water, the water tends to bleed around the aggregate particles. The amount of bleed water is highest on the surface of the aggregate and decreases with distance from it. If the aggregate has high absorption capacity, then it starts to draw water into its pores. As the water film around the aggregate is reduced, more water is drawn from the paste surrounding the aggregate towards the surface. This process continues until the aggregate is saturated. The water film around the aggregate may or may not be completely eliminated, but the water content at 10 μm and farther from the aggregate will be reduced such that the w/c in this region becomes lower than the w/c used in the mixture proportioning. The effect of absorption seems to increase with distance from the aggregate, as indicated by the porosity curve for the dry lightweight aggregate shown in Fig. 2. However, the influence of aggregate absorption does not appear to affect the bulk paste located 50 μm and farther from the aggregate surface, as the bulk paste for the three mortars showed same level of porosity. Thus, it can be argued that the zone of influence of the dry lightweight aggregate used in this study is confined between 10 and 50 μm from the aggregate surface. The same observation applies to prewetted lightweight aggregate, but to a lesser degree. The dense paste surrounding the ITZ for prewetted lightweight aggregate appears to extend between 15 and 40 μm from the aggregate surface. Although the aggregate was saturated with water prior to mixing, it seems that there is some water migration towards the aggregate. It is possible that, during mixing, some water escapes from the lightweight aggregate large pores due to the centrifugal force exerted by the rotary action of the mixer. Thus, the aggregate becomes partially saturated and starts drawing water from the surrounding paste. This water migration toward the lightweight aggregate decreases the porosity of the paste between 15 and 50 μm from the aggregate

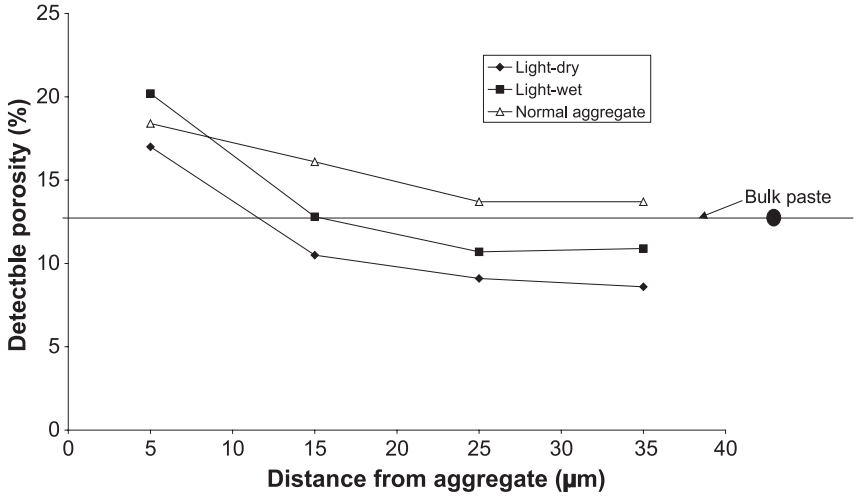

Fig. 2. Percent of detectable porosity in the successive 10-μm-wide strips around the aggregate and bulk paste for 7-day-old mortar with w/c of 0.55.

surface. For the normal aggregate, the absorption capacity is small as compared with the lightweight aggregate. Therefore, the bleed water around the aggregate cannot be removed, and the zone surrounding the aggregate will have higher a w/c than the bulk paste does. Consequently, the porosity in this zone becomes higher than that of the bulk paste.

The ITZ thickness based on porosity curves appears to depend on the type and condition of the aggregate. The ITZ thickness is defined as the distance from the aggregate surface to the point where the porosity of the ITZ reaches the level observed in the bulk paste. For dry lightweight aggregate, the ITZ thickness is slightly greater than 10 μm. As for prewetted lightweight aggregate, the thickness is about 15 μm. The ITZ thickness for normal aggregate seems to extend beyond 35 μm.

The percentage of unhydrated cement (UH) around the dry and prewetted lightweight and the normal aggregates is shown in Fig. 3. The UH content of the bulk paste, which was similar for all mortars investigated, is also shown in Fig. 3 by a point outside the range of the horizontal axis. The trends previously observed for the porosity curves (Fig. 2) can be observed in the UH curves. For strips located at a distance greater than 10 μm from the aggregate surface, the dry lightweight aggregate has higher UH content than the prewetted lightweight and the normal aggregates. The UH content in the region located between 15 and 50 μm from the dry lightweight aggregate surface becomes higher than that of the bulk paste. This agrees well with the mechanism of absorption suggested in the previous paragraph. The removal of water, by absorption, from the paste surrounding the dry lightweight aggregate appears to lead to better packing of cement grains in this region. The prewetted lightweight aggregate appears to have higher UH content in the surrounding paste than the normal aggregate does. This

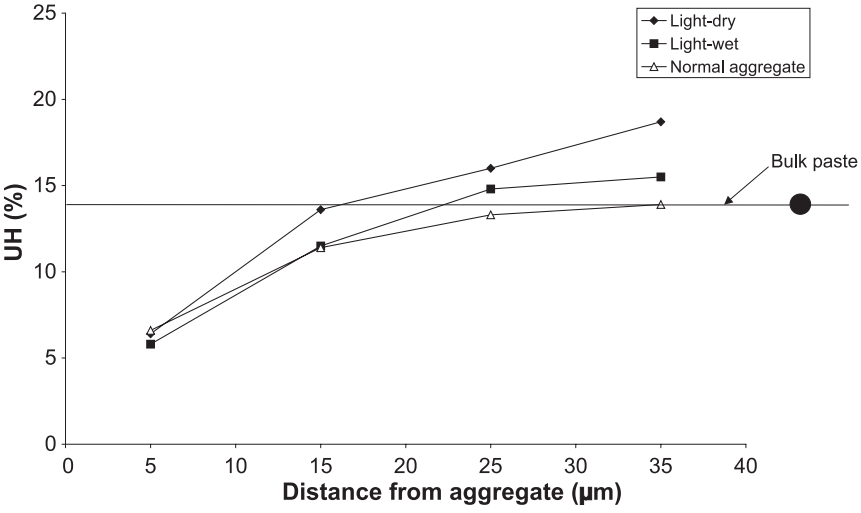

Fig. 3. Percent of unhydrated cement grains in the successive 10-μm-wide strips around the aggregate and bulk paste for 7-day-old mortar with w/c of 0.55.

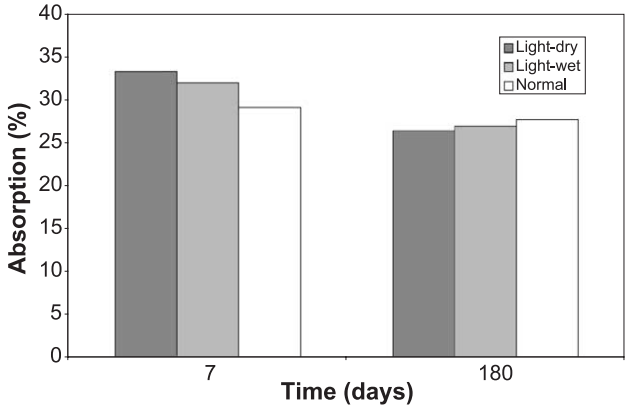

Fig. 4. Water absorption of mortar with a w/c of 0.55.

can also be attributed to the water migration toward the prewetted lightweight aggregate.

The ITZ thickness based on UH content also seems to vary according to the aggregate type and condition, as shown in Fig. 3. For dry lightweight aggregate, the ITZ thickness appears to be around 10 μm. As for prewetted lightweight aggregate, the thickness is around 20 μm. The normal aggregate ITZ thickness seems to extend to 35 μm. The ITZ, thicknesses based on porosity and on UH content appear to be identical for all aggregates investigated.

3.2. Absorption

Water absorption by vacuum saturation was used as an indicator of porosity of the mortars made with dry and prewetted lightweight aggregate, as well as normal-weight aggregate. The values of absorption for the different mortars at 7 and 180 days are shown in Fig. 4. At 7 days, both dry and prewetted lightweight aggregate mortars show higher absorption than did the mortars made with normal aggregate. This increase in porosity of lightweight mortar can be attributed mainly to the high porosity of the lightweight aggregate. At 180 days, both lightweight aggregate mortars appear to have slightly lower absorption than the normal aggregate mortar did. Thus, between 7 and 180 days, the absorption of the dry and prewetted lightweight aggregate mortars appears to have been reduced more significantly than the porosity of the normal aggregate mortar. It can be explained as follows. At 7 days, the 10-μm paste strip in the immediate vicinity of the aggregate has relatively high porosity. Thus, it is easy for the water to penetrate into the porous lightweight aggregate. After 180 days of curing, the paste in the immediate vicinity of the aggregate becomes quite dense, as shown in the BSE image given in Fig. 5. This dense paste surrounding the lightweight aggregate will seal its large pores, and hence, the porosity of the mortar will be reduced significantly.

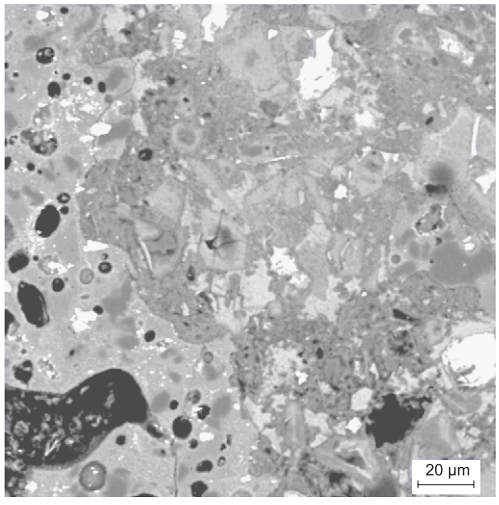

Fig. 5. Paste surrounding dry lightweight aggregate at 180 days.

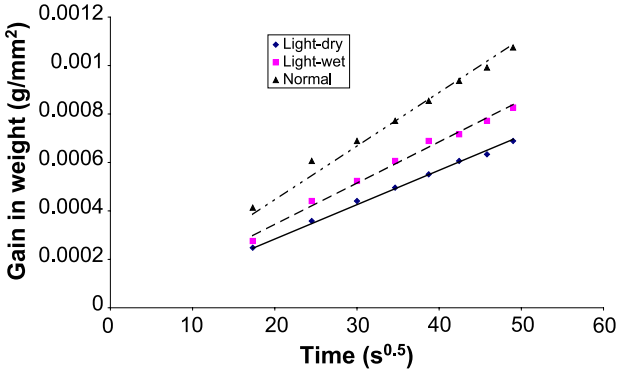

Fig. 6. Absorption versus square root of time for 180-day-old mortars with a w/c of 0.55.

3.3. Sorptivity

The absorption is plotted as function of square root of time for the three mortars and is shown in Fig. 6. The slope of the straight line that represents the relationship between absorption and square root of time is defined as sorptivity. The sorptivity of the lightweight and the normal aggregate mortars at 180 days are provided in Fig. 7. It is clearly indicated by these figures that the dry lightweight aggregate

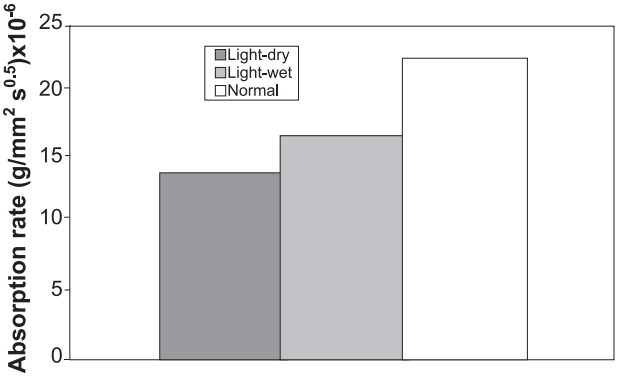

Fig. 7. Sorptivity of mortar with a w/c of 0.55 immersed in water for 180 days.

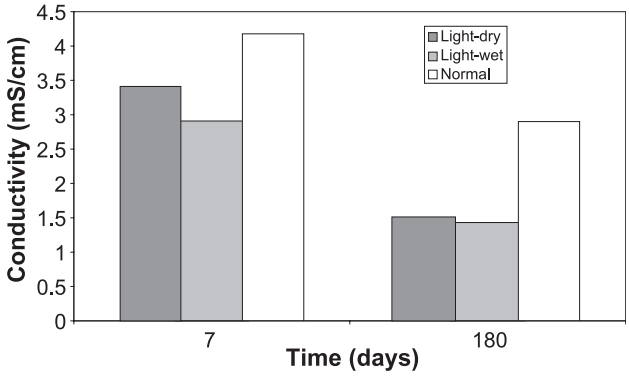

Fig. 8. Electrical conductivity for mortars with a w/c of 0.55.

mortar has the lowest sorptivity, followed by the prewetted lightweight aggregate mortar. The normal aggregate mortar has the highest sorptivity. The difference in sorptivity between the lightweight and the normal aggregate mortars may be attributed to the difference in their pores characteristics. Sorptivity is directly proportional to the velocity of capillary rise, which increases with the increase in the capillary pore size, as given in Eq. (2) [13] below:

$$V = \frac{r}{4\mu L}\gamma\cos\theta \qquad (2)$$

where V=average velocity of capillary rise of fluid; r=radius of pore; γ=surface tension; μ=viscosity of the fluid; L=capillary rise; and θ=contact angle between the fluid and solid surfaces.

Thus, based on Eq. (2), upon contact with the water, the empty large pores will start drawing water at a faster rate than smaller pores do. This may indicate that lightweight aggregate mortars possess smaller capillary pores than normal aggregate mortars do, as the former have lower sorptivity than the latter do. This result is in agreement with the microstructural observations that indicated that the ITZ surrounding the normal aggregate is more porous and thicker than that surrounding the lightweight aggregate. Thus, more large pores may exist around the normal aggregate than around the lightweight aggregate. The lightweight aggregate particles themselves contain very large pores as compared with cement paste, but these pores are not continuous and they are sealed off by the dense paste surrounding the aggregate. Therefore, their contribution to the sorptivity is not significant.

3.4. Electrical conductivity

The electrical conductivity values for the dry and prewetted lightweight and the normal aggregate mortars at 7 and 180 days are shown in Fig. 8. At 7 days, both lightweight aggregate mortars appears to have lower conductivity than the normal aggregate mortar does. The same trend is observed at 180 days. This again can be attributed to the dense ITZ in the lightweight aggregate mortar as compared with the porous ITZ in the normal aggregate mortar. Again, the pores in the lightweight aggregate do not appear to contribute significantly to the electrical conductivity, as they are sealed off by the dense paste surrounding the ITZ and they do not form continuous path for the chloride ions penetration. By comparing the values of porosity as indicted by water absorption (Fig. 4) and electrical conductivity (Fig. 8), it can be argued that overall porosity is not the sole parameter influencing conductivity, but the pore size, distribution and continuity have important influence as well.

3.5. Sulfate attack

The expansion strain of lightweight and normal aggregate mortars prisms immersed in sodium sulfate is shown in Fig. 9 as a function of exposure time. The normal aggregate

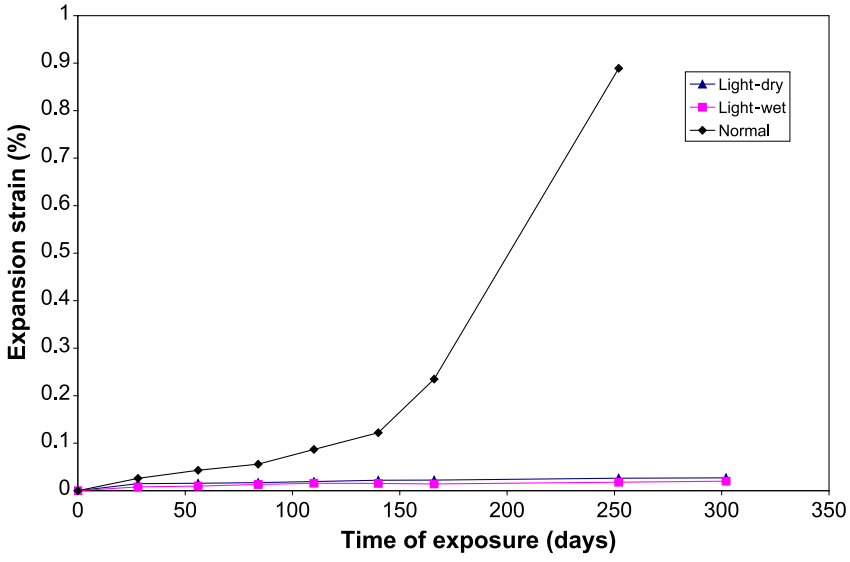

Fig. 9. Expansion strain of mortar prisms with a w/c of 0.55 exposed to 5% Na_2SO_4 solution.

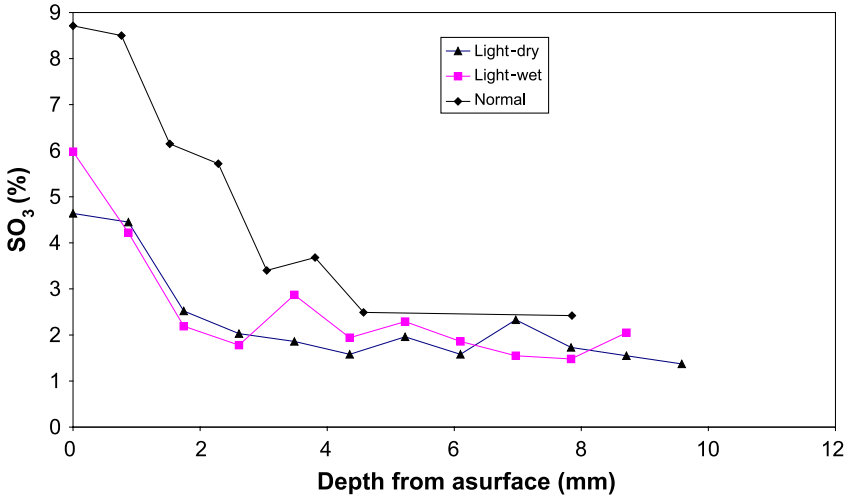

Fig. 10. SO_3 concentration profile for 168-day-old mortar with a w/c of 0.55.

mortar appears to develop significant expansion at about 140 days, and then the expansion rate seems to accelerate until the strain reaches 1% at around 250 days. As for dry and prewetted lightweight aggregate mortars, it appears that they are not experiencing significant expansion up to 300 days. The expansion of the normal aggregate mortar is due to the formation of ettringite, which is directly related to the amount of sulfate that has penetrated to the interior of the specimen. The amount of sulfate that has penetrated into the specimen was measured by the EDS. The SO_3 concentration profiles in the three mortars, obtained by EDS, after 168 days of exposure to 5% Na_2SO_4 solution are shown in Fig. 10. The normal aggregate mortar seems to have higher SO_3 concentration than do the lightweight aggregate mortars up to a depth of about 5 mm. The dry and prewetted lightweight aggregate mortars have similar SO_3 concentration profiles, except for the sampling area on the external layer where the SO_3 concentration in the prewetted lightweight aggregate mortar is slightly higher than that of the dry lightweight mortar. The diffusion of sulfate ions into the normal aggregate mortar appears to be accelerated probably by the presence of the porous ITZ around the aggregate. On the other hand, the dense ITZ around the lightweight aggregate appears to have increased the resistance of the mortar to sulfate attack. This agrees well with the results of the sorptivity and electrical conductivity tests.

Finally, the dynamic moduli are shown as functions of exposure time of the mortars stored in 5% Na_2SO_3 solution in Fig. 11. The normal aggregate mortar started experiencing reduction in dynamic modulus at around 150 days. On the other hand, the dry and prewetted lightweight aggregate mortars do not show any reduction in their dynamic moduli when exposed to Na_2SO_3 solution for up to 300 days. This provides another indication of the high resistance of lightweight aggregate mortar to the penetration of sulfate as compared with normal aggregate mortar.

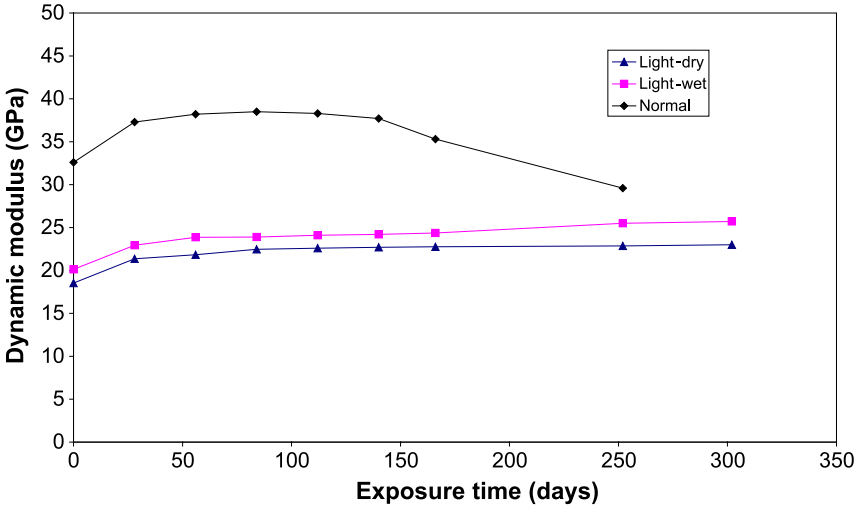

Fig. 11. Change in dynamic moduli for mortar prisms with a w/c of 0.55 exposed to 5% Na_2SO_4 solution.

4. Summary and conclusions

The results of an investigation on the effect of aggregate type and its moisture condition on the microstructure and properties of mortar are presented in this paper. Dry and prewetted lightweight aggregate, as well as normal aggregate, were investigated. The microstructure of the paste surrounding the dry and prewetted lightweight aggregate, as well as normal aggregate, was characterized by quantifying the porosity and UH content in successive 10-μm-wide strips surrounding the aggregate particle. The porosity of mortars made from the three different aggregates was determined by measuring the water absorption of specimens under vacuum saturation. Sorptivity and electrical conductivity were also measured and compared. Finally, the resistance of lightweight aggregate mortars and normal aggregate mortar to sulfate attack was investigated. The following conclusions are drawn from the results obtained in this study:

1. The ITZ around the lightweight aggregate appears to be about 10 and 15 μm thick for dry and prewetted lightweight aggregates, respectively. As for normal aggregate, the ITZ extends beyond 35 μm. The paste located between 10 and 50 μm from the surface of the lightweight aggregate seems to be denser than the bulk paste located at 50 μm and farther. This is probably due to the absorption of water by the lightweight aggregate. This result is somewhat different from the results reported by other researchers that the paste in contact with the lightweight aggregate surface is quite dense. However, these previously reported results were qualitative in nature, based on visual observation, unlike the results reported in this study, which is based on quantitative analysis.
2. The results indicate that soaking the lightweight aggregate prior to mixing does not appear to have a significant effect on the microstructure of the ITZ surrounding the aggregate as compared with dry lightweight aggregate. This may be due to the removal of water from the large pores of the prewetted lightweight aggregate by the forces exerted on the aggregate during the mixing process. The partially saturated lightweight aggregate appears to absorb water and modify the surrounding paste microstructure in a manner similar to the dry one.
3. The porosity of lightweight aggregate mortars, as indicated by water absorption under vacuum saturation, was shown to be higher than that of the normal aggregate mortar. This can be attributed to the presence of large pores in the lightweight aggregate. The pores in the lightweight aggregate may not form a fully continuous system with the pores in cement paste. However, under vacuum saturation conditions, whatever little connection between the pores in cement paste and lightweight aggregate might be sufficient to allow water to penetrate into and saturate the pores inside the lightweight aggregate particles.
4. The sorptivity and electrical conductivity of lightweight aggregate mortar is lower than that of the normal aggregate mortar. The reduction in the values of these transport properties can be attributed to the dense paste located between 10 and 50 μm from the surface of the lightweight aggregate. The high porosity of the lightweight aggregate does not appear to increase the transport properties because it is sealed by the dense ITZ.
5. The lightweight aggregate mortar showed better resistance to sulfate attack than the normal aggregate mortar did. This appears to be due to the dense microstructure of the paste surrounding the lightweight aggregate, which makes it difficult for the sulfate ion to ingress into the interior of the mortar.

References

[1] M. Zhang, O.E. Giorv, Backscattered electron imaging on the interfacial zone between high strength lightweight aggregate and cement paste, Adv. Cem. Res. 2 (1989) 141–146.
[2] M. Zhang, O.E. Giorv, Microstructure of the interfacial zone between lightweight aggregate and cement paste, Cem. Concr. Res. 20 (1990) 610–618.
[3] R. Wasserman, A. Bentur, Interfacial interaction in lightweight aggregate concretes and their influence on the concrete strength, Cem. Concr. Compos. 18 (1996) 67–76.
[4] R. Wasserman, A. Bentur, Effect of lightweight fly ahs aggregate microstructure on the strength of concretes, Cem. Concr. Res. 27 (1997) 525–537.
[5] S.L. Sarkar, S. Chandra, L. Berntsson, Interdependence of microstructure and strength of structural lightweight aggregate concrete, Cem. Concr. Compos. 14 (1992) 239–248.
[6] Y. Lo, X.F. Gao, A.P. Jeary, Microstructure of pre-wetted aggregate on lightweight concrete, Build. Environ. 34 (1999) 759–764.
[7] T.A. Holm, T.W. Bremner, J.B. Newman, Lightweight aggregate concrete subject to severe weathering, ACI Concr. Int. 6 (1984) 49–54.
[8] J. Punkki, O.E. Gjørv, Effect of water absorption by aggregate on properties of high-strength lightweight concrete, in: I. Holand (Ed.), International Symposium on Structural Lightweight Aggregate Concrete, Norwegian Concrete Association, Sandfjord, 1995, pp. 604–616.
[9] J. Punkki, O.E. Gjørv, P.J. Monteiro, Microstructure of high-strength lightweight aggregate concrete, in: F. de-Larrard, R. Lacroix (Eds.), 4th Int. Symposium on Utilization of High-strength/High-performance Concrete, F. Presses de 1ÕENPC, Paris, France, 1996, pp. 1281–1287.
[10] K.S. Chia, M. Zhang, Water permeability and chloride penetrability of high-strength lightweight aggregate concrete, Cem. Concr. Res. 32 (2001) 1–7.
[11] A. Elsharief, M.D. Cohen, J. Olek, Influence of aggregate size, water cement ratio and age on the microstructure of the interfacial transition zone, Cem. Concr. Res. 33 (11) (2003) 1837–1849.
[12] P.E. Streicher, G.M. Alexander, A chloride conduction test for concrete, Cem. Concr. Res. 25 (1995) 1284–1294.
[13] N.S. Martys, C.F. Ferraris, Capillary transport in mortars and concrete, Cem. Concr. Res. 27 (1997) 747–760.